

REPORTS

- to 18% (w/w) glucose and 40 to 55% (w/w) sucrose]. The viscosity of each solution was measured with a viscometer and was adjusted by varying the sugar concentrations. The experiments were performed at room temperature ($\sim 23^\circ\text{C}$).
14. We used a Nikon $\times 60$, 1.2 numerical aperture water immersion objective, a Zeiss 60-mm-to-infinity-corrected conversion lens, a $\times 0.25$ Zeiss tube lens, a Hamamatsu microchannel plate intensifier, and a Phillips video camera.
 15. The extension data were smoothed by Gaussian weighted averages of adjacent frames.
 16. We determined the relaxation time to be 3.9 s in a 41-cP sugar solution by observing the relaxation of stretched molecules as described previously (10). The relaxation time in the sugar solutions of other viscosities was assumed to be proportional to the ratio of the viscosities.
 17. R. Larson, T. Perkins, D. Smith, S. Chu, *Phys. Rev. E* **55**, 1794 (1997).
 18. S. B. Smith, L. Finzi, C. Bustamante, *Science* **258**, 1122 (1992); C. Bustamante, J. F. Marko, E. D. Siggia, S. Smith, *ibid.* **265**, 1599 (1994).
 19. The average extension observed at zero residence time is about $2.5\ \mu\text{m}$ (Fig. 2). The observed coil size appears larger than the known size of about $1.4\ \mu\text{m}$ (twice the radius of gyration) because of a blooming effect in the intensified video camera when objects of saturating brightness were imaged [D. E. Smith, T. T. Perkins, S. Chu, *Macromolecules* **29**, 1372 (1996); *Phys. Rev. Lett.* **75**, 4146 (1995)]. The same effect was noted previously [S. B. Smith, P. K. Aldridge, J. B. Callis, *Science* **243**, 203 (1989)] and must be kept in mind when analyzing the data.
 20. E. Hinch, *J. Non-Newtonian Fluid Mech.* **34**, 181 (1994).
 21. R. Larson, in preparation.
 22. See, for example, P. Flory, *Statistical Mechanics of Chain Molecules* (Interscience, New York, 1969).

23. See R. G. Winkler, P. Reineker, M. Schreiber, *Europhys. Lett.* **8**, 493 (1989) for an attempt to calculate the entropic elastic forces dynamically. However, this model does not consider the dynamics in flow or allow for features such as folds.
24. E. W.-G. Diau, J. L. Herek, Z. H. Kim, A. H. Zewail, *Science* **279**, 847 (1998).
25. J. N. Onuchic, Z. Luthey-Schulten, P. G. Wolynes, *Annu. Rev. Phys. Chem.* **48**, 539 (1997).
26. We acknowledge assistance from H. Babcock, W. Fann, R. Larson, T. Perkins, and W. Volkmuth. This work was supported in part by the U.S. Air Force Office of Scientific Research, National Science Foundation (NSF), the Human Frontiers Foundation, and by an endowment established by Theodore and Frances Geballe. D.E.S. was supported by a fellowship from the NSF Program in Mathematics and Molecular Biology.

28 May 1998; accepted 23 July 1998

Three-Dimensional Deformation Measured in an Alaskan Glacier

Joel T. Harper, Neil F. Humphrey, W. Tad Pfeffer

Measurements of movement along 28 boreholes reveal the three-dimensional flow field in a 6 million cubic meter reach of Worthington Glacier, a temperate valley glacier located in Alaska. Sliding at the bed accounted for 60 to 70 percent of the glacier's surface motion. Strain rates in the ice were low from the surface to a depth of about 120 meters, but then increased rapidly toward the bed. Ice deformation was not affected by temporal changes in the sliding rate. The three-dimensional pattern of motion indicates that plane strain, which is often assumed by models, is a poor approximation of this viscous flow.

All models for glacier motion, whether their purpose is to calculate a timeline for an ice core or to test the stability of the West Antarctic Ice Sheet, must call on various assumptions about the relations between the stresses acting on the ice body and the flow field that results. Yet, many of these relations have not been well documented with observation or laboratory measurements (1). For example, the surface velocity of glaciers can change over hours, days, or seasons—sometimes affecting the entire glacier and other times only small reaches (2). While nonsteady sliding processes at the bed are typically cited as an explanation for this variability (3), little is known about the spatial and temporal structure of internal deformation of glaciers and ice sheets. We thus measured the three-dimensional flow field within a large reach of Worthington Glacier, a temperate valley glacier located in the Chugach Mountains, Alaska (Fig. 1). Instruments were arranged on the reach—which has a volume of $6.2 \times 10^6\ \text{m}^3$ and extends 230 m in length, 150 m in width, and 180 to 200 m in depth—to image the glacier's short-term three-dimensional velocity

field. The spacing of the measurement points in all three dimensions was much less ($<10\%$) than the ice thickness. These data offer a means for understanding the details of deformation and sliding processes.

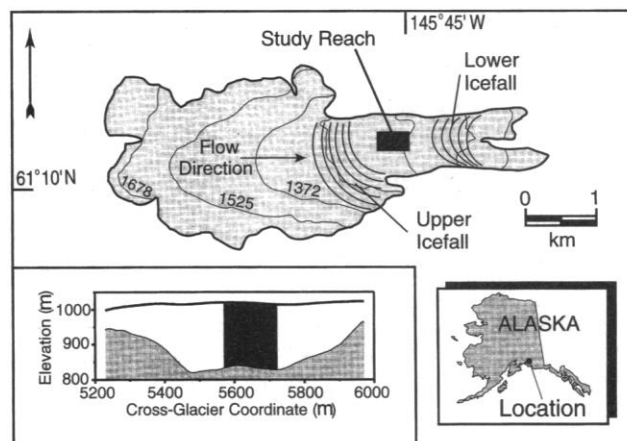
The measured reach is just below the dividing line between the accumulation and ablation areas of the glacier. Radio-echo sounding measurements indicate that the area surrounding the study reach has steep valley walls, a relatively flat valley floor, and a maximum thickness of just over 200 m (4). Located about 200 m up-glacier and 300 m down-glacier from the

reach are two icefalls, each of which drops more than 300 m vertically and is extensively crevassed. The average surface slope is 2° to 3° in the study reach, closer to 10° when averaged along the length of the glacier, and 20° to 25° through the icefalls.

The velocity field was determined by measuring the displacement over time of a network of surface markers and a vertical array of points along 28 boreholes drilled to depths of 180 to 200 m. The boreholes were drilled with a hot water system using instrumentation and methods designed to create straight holes with uniform and smooth walls. The holes were inspected for smoothness with a video camera (5) and were not fitted with casing. Most holes were drilled to about 10 m above the glacier bed so that no connection was made with the basal hydrologic system, which would have altered the drainage system and thermally eroded the holes. The boreholes were repeatedly measured with an inclinometer that quantifies both tilt and azimuth orientation of points along the hole, thus giving its full three-dimensional trajectory.

The boreholes were spaced about 20 m apart along the glacier and 30 m apart across the glacier. Data were collected at 2-m vertical intervals in each borehole. Markers and borehole trajectories were surveyed four separate

Fig. 1. The location of Worthington Glacier and the study reach. Inset in lower left shows a cross-sectional profile of the glacier extending through the study reach; the lower line is bed, the upper line is the ice surface, and the dark block is the study reach.



J. T. Harper and N. F. Humphrey, Department of Geology and Geophysics, University of Wyoming, Laramie, WY 82071, USA. W. T. Pfeffer, Institute of Arctic and Alpine Research, University of Colorado, Boulder, CO 80309, USA.

REPORTS

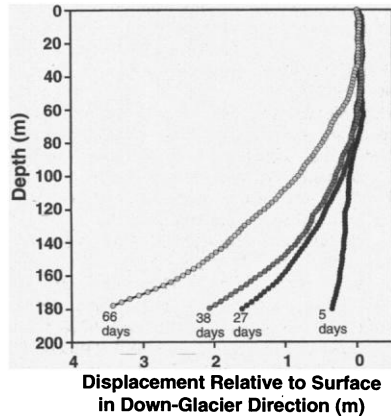


Fig. 2. Deformation of a borehole in the along-glacier plane. The borehole is displayed at four time steps with each trajectory showing the relative displacement of points along the hole with respect to the top of the borehole.

times over a period of 60 to 70 days (depending on the borehole) between May and August. By the end of the study period the total horizontal displacements were about half of the initial horizontal spacings of markers and boreholes. These data therefore give an image of the flow field that is averaged over length scales of about 10 to 15 m horizontally and 1 m vertically.

The trajectory of each borehole was measured at least twice during each time interval and the measurements were then averaged. We were able to construct the projection of the boreholes from unsmoothed inclinometry data. Such an approach is in contrast to previous borehole deformation studies (6). Statistical analysis suggests that measurement errors in the trajectories increase away from the surface, but that the bottom of the boreholes can be located relative to the surface to better than ± 0.19 m (7).

Because englacial displacements were not measured parallel to the length of the boreholes, vertical velocities were calculated as a residual based on the condition of incompressibility of

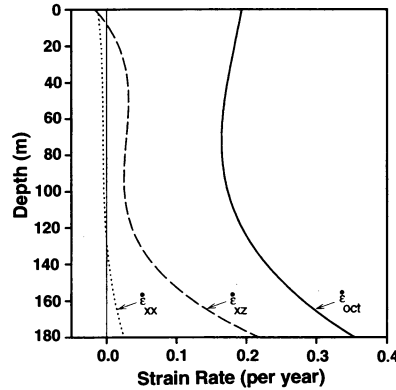


Fig. 4. Average values within the study reach of the octahedral (ϵ_{oct}), longitudinal (ϵ_{xx}), and vertical shear (ϵ_{xz}) components of the strain rate tensor (coordinate system is right handed, where x = down-glacier, y = cross-glacier, z = vertical).

the study reach (8). This technique yields the complete velocity vector at discrete locations along the borehole traces. Values at about 5000 such locations were then interpolated to form a three-dimensional gridded velocity field (9).

Internal ice deformation led to displacements between the tops and bottoms of the boreholes of 3 to 3.5 m over 60 days (Fig. 2). During the measurement period we observed the surface velocity to vary over time scales ranging from days to months (10); however, there were no significant changes in the deformation rate of the boreholes when sampled at week to month intervals. These data imply that the sliding rate at the bed of the glacier changes without influencing the rate of internal deformation of the ice above. By projecting the borehole deformation profiles 10 to 15 m to the glacier bed, we estimate that the sliding velocity accounted for 60 to 70% of the total surface motion. This is in agreement with one direct measurement of the sliding rate made with a borehole video camera (11). Sliding thus dominated the total velocity field, even though the surface slope of the glacier across the reach is low.

Velocities in the reach ranged from about 50 m/year near the bed, to about 86 m/year at the surface during our study (Fig. 3). The vertical and cross-glacier components of this motion were an order of magnitude less than the down-glacier-directed flow. Most of the flow was parallel to the bed, with gradients in velocity greatest within 60 m of the bed. Closer to the surface, the up-glacier and down-glacier edges of the reach moved slightly faster than its central portion. The regions of higher velocity may be associated with the icefalls located up-flow and down-flow from the study reach. Surface velocities near these icefalls were 30 to 40% higher than across the reach. Curiously, the regions of faster flow in the reach were restricted to the upper 50 to 75 m of the ice thickness.

The six independent components of the second rank strain-rate tensor were interpolated at discrete nodes spaced at 10 m by 15 m by 1 m within the reach. The reach-averaged octahedral, longitudinal, and vertical shear components of strain rate are displayed as a function of depth in Fig. 4. All components showed a relatively small magnitude from the surface down to a depth of about 120 m, but then increased rapidly toward the bed. Vertical shear composed only about half of the octahedral strain rate, indicating that the sum of the other components of the strain rate tensor make up as much as half of the total deformation. Thus, a simple plane strain model for flow does not fit our data, even though the study reach is located near the centerline of a relatively straight valley glacier with a width equal to four to five times its depth.

Our data indicate that the three-dimensional velocity field within this viscous flow has a complex pattern, despite the fact that its bounding geometry is relatively simple. These findings illustrate the shortcomings of many models in adequately describing the internal deformation of glaciers and ice sheets, and possibly many other viscous flows. However, small temporal variations in deformation do not appear to be present, which significantly reduces the level of complexity required to model this motion.

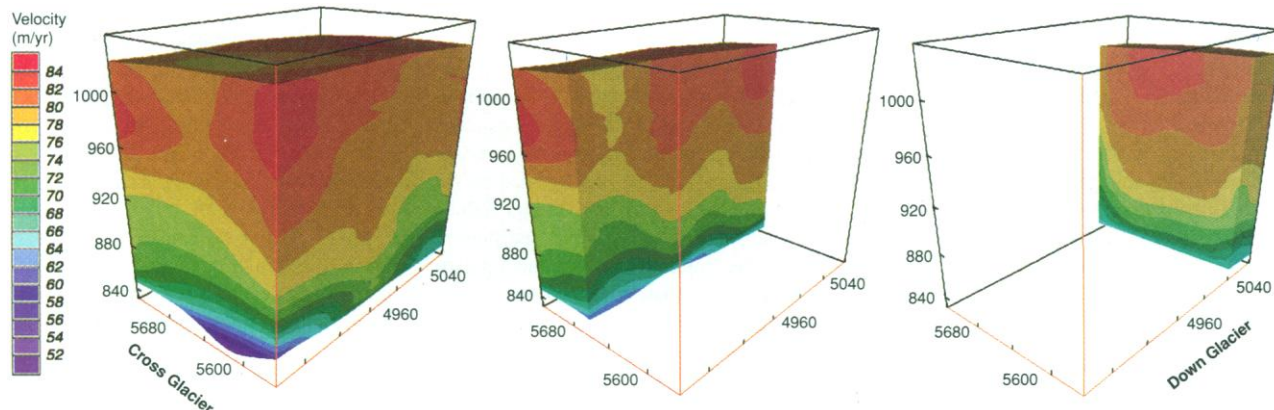


Fig. 3. Three perspective views of the total velocity field. Axes represent down-glacier, cross-glacier, and vertical coordinates of the study reach (units in meters); colors show velocity regions. Flow

parallel to the bed is visible in each view, as are the near surface regions of higher velocity along the up-glacier and down-glacier corners of the reach.

References and Notes

1. J. F. Nye, *R. Soc. London Proc. Ser. A* **219**, 477 (1953); R. LeB Hooke, *Rev. Geophys. Space Phys.* **19**, 664 (1981); C. J. van der Veen and I. M. Whillans, *J. Glaciol.* **36**, 324 (1990).
2. Examples include velocity variations occurring over months to weeks [R. LeB Hooke, P. Calla, et al., *J. Glaciol.* **35**, 235 (1989)] and days to hours [A. Iken and R. A. Bindshchadler, *ibid.* **32**, 101 (1986)].
3. S. M. Hodge, *ibid.* **13**, 349 (1974); B. Kamb et al., *J. Geophys. Res.* **99**, 15231 (1994); J. Harbor et al., *Geology* **25**, 739 (1997).
4. A dense array of radio-echo sounding measurements were processed with three-dimensional migration techniques. Comparisons of these measurements with borehole observations suggest that the radar is accurate to within about 8.5 m (B. C. Welch, W. T. Pfeffer, J. T. Harper, N. F. Humphrey, *J. Glaciol.*, in press).
5. J. T. Harper and N. F. Humphrey, *Geology* **23**, 901 (1995).
6. M. F. Meier, *U.S. Geol. Surv. Prof. Pap.* 351 (1960); W. S. B. Paterson and J. C. Savage, *J. Geophys. Res.* **68**, 4537 (1963); C. F. Raymond, *J. Glaciol.* **10**, 55 (1971); R. LeB. Hooke, P. Holmlund, N. R. Iverson, *ibid.* **33**, 72 (1987) were all forced to smooth inclinometry data because of high levels of noise.
7. The instrument was constructed by Slope Indicator Canada, Ltd. (Vancouver, BC). Measurement errors associated with a prototype of this instrument are discussed by E. W. Blake and G. K. C. Clarke [*J. Glaciol.* **38**, 113 (1992)]. However, analysis of actual data from the instrument used suggests that instrument errors are slightly improved from manufacturer specifications [J. T. Harper, thesis, University of Wyoming (1997); S. V. Huzurbazar, unpublished material]. Additionally, the uniformity of the borehole walls enabled a high degree of repeatability for the measurements.
8. We follow the method of C. F. Raymond, *J. Glaciol.* **10**, 39 (1971).
9. We use a cubic spline function with an iterative scheme designed to minimize the curvature of the function between data points [I. C. Briggs, *Geophysics* **1974**, 39 (1974)]. This interpolation was tested extensively with synthetic data.
10. J. T. Harper, N. F. Humphrey, W. T. Pfeffer, B. C. Welch, *U.S. Army Cold Reg. Res. Eng. Lab. Spec. Rep.* 96-27 (1996), p. 41.
11. This measurement was made within the same reach and time of year as the deformation experiments, but during a subsequent year. Sliding and surface velocities were determined by continuous filming of the base of a borehole with concurrent surveying of velocity at the surface.
12. Funded by grants from NSF (OPP-9122966 to N.F.H. and OPP-9122916 to W.T.P.). Additional funding for computer visualization was provided by NSF's EPSCoR (Experimental Program to Stimulate Competitive Research) program (EPS9550477), through the University of Wyoming's Spatial Data and Visualization Center project. D. Bahr, B. Welch, and B. Raup all made significant contributions to portions of the work presented here.

16 April 1998; accepted 28 July 1998

A Neoproterozoic Snowball Earth

Paul F. Hoffman,* Alan J. Kaufman, Galen P. Halverson, Daniel P. Schrag

Negative carbon isotope anomalies in carbonate rocks bracketing Neoproterozoic glacial deposits in Namibia, combined with estimates of thermal subsidence history, suggest that biological productivity in the surface ocean collapsed for millions of years. This collapse can be explained by a global glaciation (that is, a snowball Earth), which ended abruptly when subaerial volcanic outgassing raised atmospheric carbon dioxide to about 350 times the modern level. The rapid termination would have resulted in a warming of the snowball Earth to extreme greenhouse conditions. The transfer of atmospheric carbon dioxide to the ocean would result in the rapid precipitation of calcium carbonate in warm surface waters, producing the cap carbonate rocks observed globally.

During the 200 million years (My) preceding the appearance of macroscopic metazoans, ~750 to 550 million years ago (Ma) (1), the fragmentation of a long-lived supercontinent (2) was accompanied by intermittent, but widespread, glaciation (3–5). Many of the glacial deposits contain carbonate debris or are directly overlain by carbonate rocks (6, 7), including inorganic sea-floor precipitates, which are normally limited to warm-water settings (8). Post-glacial carbonate rocks (cap carbonates) occur even in terrigenous-dominated sections (6, 7). Certain glacial units contain large sedimentary iron formations (9), which reappear after a 1-billion-year hiatus in the stratigraphic record. The glacial intervals are spanned by decreases of as much as 14 per mil in the $\delta^{13}\text{C}$ value of the surface ocean (10, 11). These isotopic excursions are enormous in comparison with any

excursions in the preceding 1.2 billion years (12) or in the Phanerozoic eon (13).

Paleomagnetic evidence suggests that the ice line reached sea level close to the equator during at least two Neoproterozoic glacial episodes (14). The origin of these extreme glaciations has been controversial (1, 15, 16). Kirschvink (17) proposed a snowball Earth, created by a runaway albedo feedback, in which the world ocean was virtually covered by sea ice but continental ice cover was thin and patchy because of the virtual elimination of the hydrologic cycle. Kirschvink applied this hypothesis to explain the low-paleolatitude glacial deposits as well as the occurrence of banded iron formations, suggesting that an ocean sealed by sea ice would quickly become anoxic and rich in dissolved ferrous iron (17). Here, we present new data on the amplitude, timing, and duration of inorganic $\delta^{13}\text{C}$ variations in Neoproterozoic rocks of northern Namibia and the relation between these variations and glaciation. We show that the snowball Earth hypothesis best explains the geological and geochemical observations, including the $\delta^{13}\text{C}$ excursions and the existence of carbonates immediately following glaciations.

We studied the Otavi Group (Fig. 1), a carbonate platform covering the southern promontory of the Congo Craton in northern Namibia (15, 18, 19). In the late Neoproterozoic, the Congo Craton was a Bahama-type sea-level platform that was about the size of the conterminous United States. Paleomagnetic data from the eastern part of the craton (20) imply that the Otavi Group was at ~12°S paleolatitude at 743 ± 30 Ma and at ~39°S at 547 ± 4 Ma. The Otavi Group contains two discrete glacial units (Chuos and Ghaub formations) of Sturtian (~760 to 700 Ma) age (15, 19). Both units are underlain by thick carbonate successions with high $\delta^{13}\text{C}$ values, and both units are overlain by distinctive cap carbonates, recording negative $\delta^{13}\text{C}$ excursions (10, 11).

The younger of the two glacial units (the Ghaub Formation) is represented by unstratified diamictites, debris flows, and, at the top, varve-like detrital couplets crowded with ice-rafted dropstones (15). Both the onset and the termination of glaciogenic sedimentation were abrupt. The glacial deposits are composed predominantly of dolomite and limestone debris derived from the underlying Ombaatjie platform (Fig. 1). Clast and matrix lithologic compositions covary; thus, we interpreted the matrix as being detrital in origin and not as a seawater proxy. Glacial deposits on the platform are thin and highly discontinuous (not due to subsequent erosion). Alternately grounded and floating sea ice caused large horizontal plates to be detached from the directly underlying bedrock. The subglacial erosion surface has remarkably little relief on the platform (~50 m relative to underlying strata over a distance of 150 km), suggesting that any fall in relative sea level was limited or short-lived. Comparatively thick sections (<180 m) of diamictites and debris flows occur on the continental slope, suggesting that the ice grounding line remained close to the platform edge (Fig. 1). These observations are consistent with an abrupt development and a subsequent dissipation of grounded sea ice on a tropical or sub-

P. F. Hoffman, G. P. Halverson, D. P. Schrag, Department of Earth and Planetary Sciences, Harvard University, Cambridge, MA 02138, USA. A. J. Kaufman, Department of Geology, University of Maryland, College Park, MD 20742, USA.

*To whom correspondence should be addressed. E-mail: hoffman@eps.harvard.edu